

Enhanced photoluminescence of heavily *n*-doped germanium

M. El Kurdi,^{1,a)} T. Kociniewski,¹ T.-P. Ngo,¹ J. Boulmer,¹ D. Débarre,¹ P. Boucaud,^{1,b)} J. F. Damlencourt,² O. Kermarrec,³ and D. Bensahel³

¹Institut d'Electronique Fondamentale, CNRS—Univ Paris-Sud 11, Bâtiment 220, 91405 Orsay, France

²CEA-DRT-LETI, 17 rue des martyrs 38054 Grenoble Cedex 9, France

³STMicroelectronics, Rue Jean Monnet 38054 Crolles, France

(Received 2 April 2009; accepted 27 April 2009; published online 14 May 2009)

We show that a significant enhancement of the direct band gap photoluminescence can be achieved at room temperature in bulk Ge and Ge-on-insulator heavily *n*-doped by gas immersion laser doping. The photoluminescence signal from bulk Ge and Ge-on-insulator increases with the donor concentration. An enhancement factor of 20 as compared to the undoped material is achieved near the 1550 nm wavelength for active dopant concentrations around $5 \times 10^{19} \text{ cm}^{-3}$. These results are supported by calculations of the Ge spontaneous emission spectrum taking into account the doping effect on the electron distribution in the direct and indirect conduction band valleys. © 2009 American Institute of Physics. [DOI: 10.1063/1.3138155]

Germanium is a promising material to achieve laser emission on a silicon platform. Germanium exhibits a direct band gap at 1550 nm at room temperature. Since the direct conduction valley of germanium is at an energy of 136 meV above the indirect conduction *L* valley,¹ the direct band gap recombination intensity is limited by carrier thermalization into the indirect conduction *L* valleys. Two approaches have been proposed to overcome this intrinsic limitation. In one approach, the reduction of the energy difference between direct and indirect band gaps can be obtained by applying a tensile strain to germanium.² It has been shown theoretically that Ge can become a direct band gap material under a 2% tensile strain.^{2–4} However the direct band gap shrinks to 0.4 eV at this strain magnitude, corresponding to a 2.5 μm emission wavelength. In order to keep the emission near the 1550 nm wavelength, a second approach has been proposed to compensate the energy difference between Γ and *L* valleys by *n*-doping of Ge.⁵ The incorporation of *n*-type dopants in germanium allows to fill the indirect conduction valley in order to enhance the carrier injection efficiency in the direct conduction band under an external pumping. For relaxed bulk Ge, a *n*-type dopant concentration of typically 10^{20} cm^{-3} results in a conduction band Fermi level energy close to the direct band edge at room temperature.

Waveguiding structures can be obtained with germanium-on-insulator (GeOI) on silicon.⁶ Recently, we have shown that GeOI substrates can be patterned into two-dimensional photonic crystals, demonstrating the interest of these substrates for photonic applications.^{7,8} In this work, we show that the Ge *n*-doping allows to enhance the room temperature photoluminescence around 1550 nm of Ge and GeOI samples. In both cases, the *n*-doping of Ge is achieved by the gas immersion laser doping (GILD) process. Experimental results are supported by the calculation of the direct radiative recombination rates of Ge as a function of the donor concentration.

The GILD technique is an *in situ* technique that has been developed to realize ultrashallow, highly doped and well ac-

tivated Si junctions with boxlike profiles.⁹ Previous experiments on relaxed Ge layers grown on Si or on silicon-on-insulator have shown that GILD may be used to dope Ge with phosphorus with boxlike concentration profiles up to 10^{20} cm^{-3} .¹⁰ GILD proceeds in an ultrahigh-vacuum system and begins with the chemisorption onto the Ge surface of a precursor gas (PCl_3). An excimer laser pulse induces an ultrafast melting/solidification process over a depth mainly controlled by the laser energy density. As solidification proceeds, liquid phase epitaxy process creates a monocrystalline Ge layer where most of the dopant atoms occupy a substitutional site. The thickness of the doped zone is equal to the melted layer thickness. The whole process has been repeated up to 25 times to increase the dopant concentration. *In situ* transient reflectivity (TR) measurements at 675 nm allow to follow the melting/solidification process at each laser pulse. As shown in Fig. 1, the melting duration, which is strongly correlated with the melted depth, increases with the laser energy density above a melting threshold, which depends on the material and substrate physical properties.⁹ In the GeOI case, the energy density is limited by a damage threshold for which the liquid/solid interface reaches the buried oxide. This damage threshold is evidenced by a drastic change of the TR signal and corresponds to a melted depth equal to the

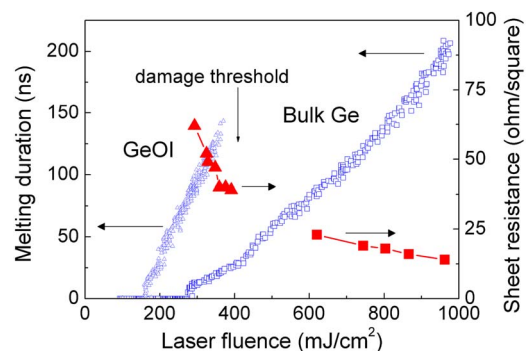


FIG. 1. (Color online) Left scale: melting duration of bulk Ge (open squares) and GeOI (open triangles) as a function of the GILD laser fluence. Right scale: sheet resistance of doped GeOI (full triangle) and bulk Ge (full squares) for 20 GILD laser shots from 290 to 390 mJ cm^{-2} and from 620 to 960 mJ cm^{-2} , respectively.

^{a)}Electronic mail: moustafa.el-kurdi@u-psud.fr.

^{b)}Electronic mail: philippe.boucaud@ief.u-psud.fr. URL: <http://pages.ief.u-psud.fr/QDgroup/index.html>.

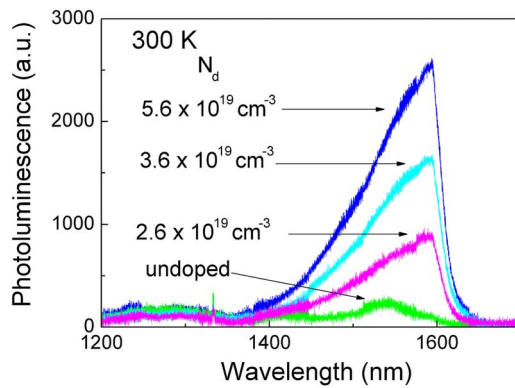


FIG. 2. (Color online) Room temperature photoluminescence spectra of phosphorus-doped bulk Ge obtained by the GILD process compared to the photoluminescence of an undoped Ge sample. The active donor concentration is indicated in the graph. The fluence is 960 mJ cm^{-2} . The detector has a cutoff at 1590 nm .

Ge thickness of the GeOI sample, i.e., 150 nm in the present case. In a first approximation, the doped layer thickness can be assumed to increase linearly from 0 to 150 nm as the laser energy density increases from the melting threshold to the damage threshold. The doping efficiency is controlled by measuring the sheet resistance of each laser doped area by the four-point-probe technique. Figure 1 also shows the sheet resistances obtained after 20 laser pulses for Ge and GeOI substrates. For both samples, the active phosphorous concentration is evaluated from the resistivity dependence on donor concentration. The photoluminescence of the doped and undoped areas is measured with a 658 nm laser diode focused on the sample surface with a 0.8 numerical aperture objective. The incident power density is typically 30 kW cm^{-2} . The photoluminescence signal is collected by the same objective and analyzed with a 0.5 m focal length monochromator coupled to a liquid nitrogen cooled multichannel InGaAs photodetector.

Figure 2 shows the photoluminescence spectra of *n*-doped germanium as compared to the photoluminescence of the undoped material. The dopant concentration N_d increases with the number of laser shots. 10, 15, and 20 shots correspond to a donor concentration N_d of $\sim 2.6 \times 10^{19}$, 3.6×10^{19} , and $5.6 \times 10^{19} \text{ cm}^{-3}$ respectively. At a 960 mJ cm^{-2} laser fluence, the depth w of the doped layer is $\sim 350 \text{ nm}$. As observed on the spectra, the photoluminescence intensity increases with the active dopant concentration. For $N_d = 5.6 \times 10^{19} \text{ cm}^{-3}$, the photoluminescence signal is enhanced by a factor 20 (10) at 1590 (1540) nm , as compared to the undoped Ge photoluminescence. The maximum of the photoluminescence spectrum is found to be at 1590 nm for doped germanium because of the detector cutoff, while it occurs at 1540 nm for the bulk material. Measurements performed with a single channel Ge detector having a longer wavelength cutoff indicate that the doped sample photoluminescence spectrum peaks at about 1610 nm . The redshift of the maximum of the doped Ge photoluminescence spectrum as compared to the undoped Ge case is attributed to the energy band renormalization in the presence of donor impurities, as shown by absorption experiments reported in Ref. 11. At very high doping densities, strain can also contribute to band gap renormalization. Meanwhile the emission broadening is significantly increased from 75 nm for undoped samples to 160 nm for doped samples. The broadening of the direct

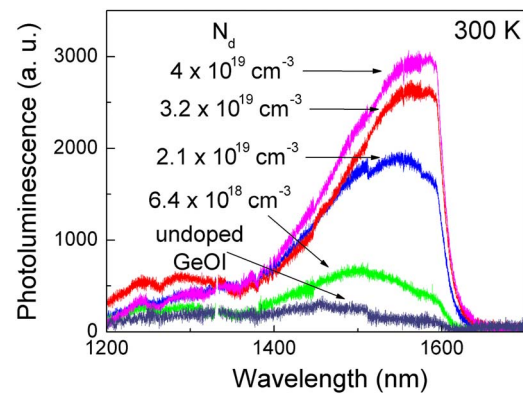


FIG. 3. (Color online) Room temperature photoluminescence spectra of phosphorus-doped GeOI sample for various doping concentrations. The photoluminescence spectrum of undoped GeOI measured in the same conditions is given for comparison. The residual signal at 1330 nm from spontaneous emission of the pumping laser was removed from the spectrum. The fluence is 350 mJ cm^{-2} .

band gap photoluminescence in *p*-doped Ge has been previously reported by Wagner and Viña¹² and described as a combination of band-to-band transitions with and without momentum conservation. Transitions without momentum conservation can be attributed to carrier scattering. The integrated photoluminescence intensity for the direct band gap recombination is enhanced by a factor 30 for $N_d = 5.6 \times 10^{19} \text{ cm}^{-3}$ as compared to undoped germanium.

The photoluminescence signal has been investigated as a function of the GILD laser fluence for a fixed number of 20 laser shots (not shown). As the laser fluence is tuned from 620 to 960 mJ cm^{-2} , the doped layer thickness increases while the donor concentration experimentally remains around $6 \times 10^{19} \text{ cm}^{-3}$. The measured photoluminescence amplitude varies linearly as a function of the laser fluence, i.e., as a function of the doped layer thickness. The extrapolation of this linear dependence to a zero photoluminescence intensity corresponds to a 280 mJ cm^{-2} laser fluence, close to the 300 mJ cm^{-2} melting threshold measured for bulk Ge (see Fig. 1).

The GILD process has been applied for doping the 150 nm thick Ge layer of a GeOI substrate with a 440 nm thick buried oxide. The melting threshold is obtained for a laser fluence of 170 mJ cm^{-2} (see Fig. 1). At a 350 mJ cm^{-2} laser fluence, the doping depth w is around 120 nm . Like for the case of bulk Ge, the dopant incorporation is mainly controlled by the number of laser shots on the sample surface. For 5, 10, 15, and 20 laser shots, the estimated active phosphorous donor concentrations N_d are 0.64×10^{19} , 2.1×10^{19} , 3.2×10^{19} , and $4 \times 10^{19} \text{ cm}^{-3}$, respectively. A comparison between the photoluminescence spectra of doped and undoped GeOI is shown in Fig. 3. As for bulk Ge, we observe that the photoluminescence signal increases with the dopant concentration. As shown in Fig. 3, an enhancement of 20 is observed at 1570 nm with a $4 \times 10^{19} \text{ cm}^{-3}$ active phosphorus concentration. In contrast to the bulk Ge situation, the GeOI photoluminescence spectrum is modified by Fabry-Perot resonances due to the air/Ge/SiO₂/Si vertical stacking. This Fabry-Perot effect reinforces the emission around 1450 nm , thus leading to a larger broadening of the emission as compared to bulk Ge case.

In order to analyze the observed enhancement of the photoluminescence intensity, we have calculated the sponta-

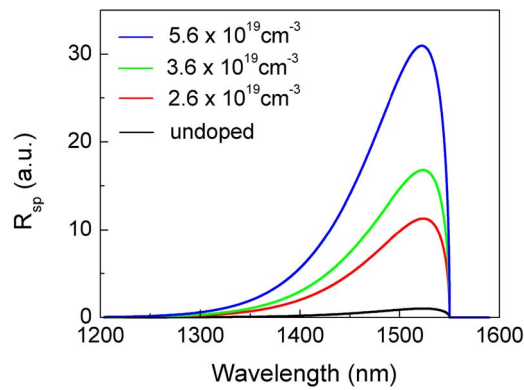


FIG. 4. (Color online) Calculated spontaneous emission spectra of undoped and n -doped Ge with different donor concentrations (from 2.6×10^{19} to 5.6×10^{19} cm^{-3}) at room temperature and for an identical excitation density. To facilitate the comparison, the maximum of the undoped sample spectrum is set equal to one. Enhancement by a factor of 30 is reached for a 5.6×10^{19} cm^{-3} active dopant concentration.

neous emission rate spectrum for the direct transition in Ge at room temperature taking into account n -doping. The spontaneous emission spectrum for direct transition R_{sp} can be expressed as $R_{\text{sp}}(h\nu) \propto (1/\tau_r) f_c(h\nu) [1 - f_v(h\nu)] \times \alpha(h\nu)$, where τ_r is the radiative lifetime, $\alpha(h\nu)$ is proportional to the absorption spectrum, and f_c and f_v are the conduction and valence Fermi–Dirac distributions at room temperature. For a direct band gap transition $\alpha(h\nu) = A \sqrt{h\nu - E_g^\Gamma}$, where E_g^Γ is the direct band gap energy (800 meV). In a first approximation, we suppose that these quantities do not depend on the carrier and impurity densities in the material. We assume parabolic bands and include both direct and indirect valleys for the calculation of the valence and conduction band quasi-Fermi levels E_{fv} and E_{fc} , respectively. The photoinduced carrier density is calculated by considering the carrier diffusion length and a lifetime limited by Auger recombination.¹³ We did not consider surface recombination or nonradiative defect recombinations since we are lacking experimental values for these parameters. The calculated emission spectra are shown in Fig. 4, for undoped Ge and doped Ge with doping

level N_d from 2.6×10^{19} to 5.6×10^{19} cm^{-3} . It is found that the spontaneous emission rates increase up to 30 times in this doping level range, which is consistent with the experimental increase of the photoluminescence signal. Note that experimentally the thickness of Ge involved in the photoluminescence is larger in the undoped sample than in the doped samples. This modeling illustrates the interest of doping to enhance the room temperature direct band gap recombination of germanium. The combination of GeOI substrates and n -type doping offers promising perspectives for light-emitting devices on a silicon platform.^{14,15}

This work was partly supported by the French Ministry of Industry under Nano2012 convention and by “Triangle de la Physique.” We thank Daniel Bouchier for fruitful discussions.

- ¹S. Richard, F. Aniel, and G. Fishman, *Phys. Rev. B* **70**, 235204 (2004).
- ²R. Soref, J. Kouvetakis, and J. Menendez, *Mater. Res. Soc. Symp. Proc.* **958**, 13 (2007).
- ³J. Menendez and J. Kouvetakis, *Appl. Phys. Lett.* **85**, 1175 (2004).
- ⁴M. El Kurdi, G. Fishman, S. Sauvage, and P. Boucaud (unpublished).
- ⁵J. Liu, X. Sun, P. Becla, L. C. Kimerling, and J. Michel, *Fifth IEEE International Conference on Group IV Photonics* (IEEE, New York, 2008), pp. 16–18.
- ⁶T. Tezuka, N. Sugiyama, and S. Takagi, *Appl. Phys. Lett.* **79**, 1798 (2001).
- ⁷M. El Kurdi, S. David, X. Checoury, G. Fishman, P. Boucaud, O. Kermarrec, D. Bensahel, and B. Ghyselen, *Opt. Commun.* **281**, 846 (2008).
- ⁸T.-P. Ngo, M. El Kurdi, X. Checoury, P. Boucaud, J. F. Damlencourt, O. Kermarrec, and D. Bensahel, *Appl. Phys. Lett.* **93**, 241112 (2008).
- ⁹G. Kerrien, T. Sarnet, D. Débarre, J. Boulmer, M. Hernandez, C. Laviron, and M. N. Semeria, *Thin Solid Films* **453**, 106 (2004).
- ¹⁰D. Cammilleri, F. Fossard, D. Débarre, C. T. Manh, C. Dubois, E. Bustarret, C. Marcenat, P. Achatz, D. Bouchier, and J. Boulmer, *Thin Solid Films* **517**, 75 (2008).
- ¹¹C. Haas, *Phys. Rev.* **125**, 1965 (1962).
- ¹²J. Wagner and L. Viña, *Phys. Rev. B* **30**, 7030 (1984).
- ¹³A. Othonos, *J. Appl. Phys.* **83**, 1789 (1998).
- ¹⁴M. El Kurdi, P. Boucaud, S. Sauvage, G. Fishman, O. Kermarrec, Y. Campidelli, D. Bensahel, G. Saint-Girons, I. Sagnes, and G. Patriarche, *J. Appl. Phys.* **92**, 1858 (2002).
- ¹⁵T. Brunhes, P. Boucaud, S. Sauvage, F. Aniel, J. M. Lourtioz, C. Hernandez, Y. Campidelli, O. Kermarrec, D. Bensahel, G. Faini, and I. Sagnes, *Appl. Phys. Lett.* **77**, 1822 (2000).